

A Yolk@Shell Nanoarchitecture for Au/TiO₂ Catalysts**

Ilkeun Lee, Ji Bong Joo, Yadong Yin, and Francisco Zaera*

Dedicated to the Fritz Haber Institute, Berlin, on the occasion of its 100th anniversary

Traditionally, gold has been considered a fairly inert metal. However, Bond^[1] and Haruta^[2,3] challenged that view a few decades ago by showing that, when dispersed as small nanoparticles, gold can catalyze several hydrogenation and oxidation reactions. Many reports have been published since on the usefulness of gold catalysis for the promotion of a wide variety of reactions.^[4,5] Unfortunately, this has not translated into many practical applications. One of the main limitations has been that supported gold catalysts are often unstable under reaction conditions: they tend to sinter and grow into larger particles, and that leads to the loss of the unique properties seen in the original nanoparticles.^[6] Although several schemes have been advanced to address this shortcoming, no satisfactory solution has been found yet. This is particularly true for the case of gold catalysts dispersed on titania, a support of interest because of its synergistic effect in further facilitating the promotion of oxidation^[7,8] and photocatalytic reactions.^[9] Here we report on the preparation and characterization of a Au@TiO₂ catalyst with a new yolk@shell nanostructure. The new catalyst shows an activity comparable to that of other more conventional Au/TiO₂ catalysts but an increased stability against sintering.

The growth of titania hollow shells encapsulating metal nanoparticles is more difficult than with silica, the material with which most reported yolk@shell nanostructures have been made to date.^[10,11] However, we have now accomplished this by following a sol–gel-based templating protocol where citrate-stabilized gold nanoparticles are first coated with a sacrificial layer of silica using tetraethyl orthosilicate (TEOS).^[12] An outer shell of titania is then grown on top using tetrabutyl titanate (TBOT), and the silica etched away using an aqueous solution of NaOH.^[12,13] The size of the void space inside the titania shells can be controlled by the amount of TEOS used during the growth of the silica layer, and the thickness of the shell by repeating the TBOT sol–gel step multiple times. Figure 1a,c displays typical transmission electron microscopy (TEM) images of the Au@TiO₂ yolk@shell nanostructure used herein, which consist of gold nano-

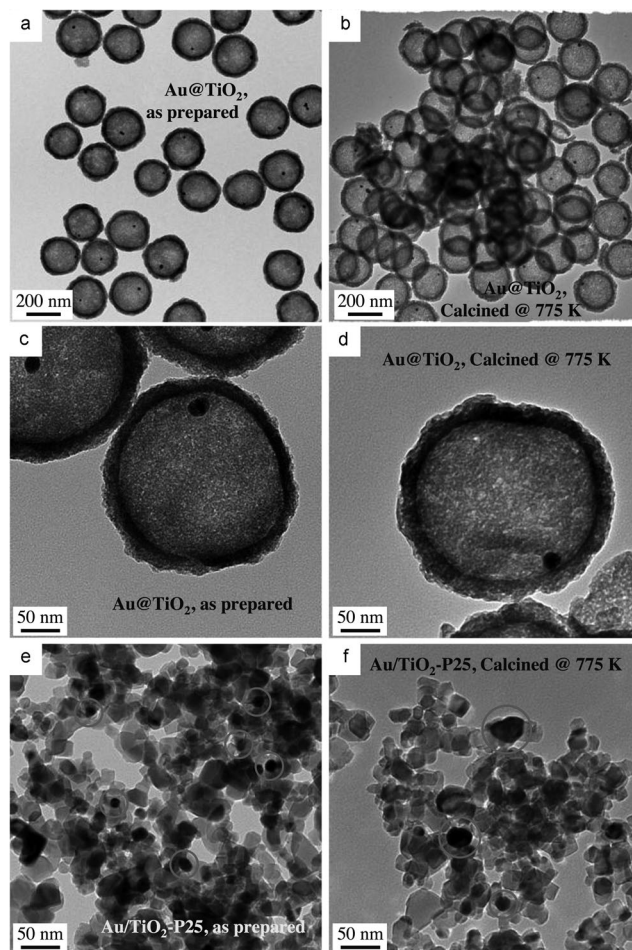


Figure 1. a,b) Low- and c,d) high-resolution TEM images of the Au@TiO₂ catalyst developed herein, and e,f) also of the 1 wt % Au/TiO₂-P25 reference sample, all shown as prepared (left-hand column: a,c,e) and after calcination at 775 K for 2 h (right-hand column: b,d,f). Sintering of some of the Au nanoparticles in the Au/TiO₂-P25 catalysts is highlighted by circles in the bottom images: e,f).

particles approximately 10 nm in diameter individually encased in titania shells approximately 200 nm in diameter and approximately 20 nm in thickness.

The accessibility of the gold nanoparticles in these Au@TiO₂ nanostructures by reactants for catalysis was assessed by in situ diffuse-reflectance infrared absorption spectroscopy (DRIFT) using carbon monoxide as a probe. The left-hand panel of Figure 2 displays IR spectra in the region of C–O bond-stretching vibrations (between 2050 and 2250 cm^{−1}) as a function of temperature for the adsorption of CO in equilibrium with gas-phase CO at 200 Torr. Two peaks

[*] Dr. I. Lee, Dr. J. B. Joo, Prof. Y. Yin, Prof. F. Zaera
Department of Chemistry, University of California
Riverside, CA 92521 (USA)
E-mail: zaera@ucr.edu
Homepage: <http://research.chem.ucr.edu/groups/zaera/>

[**] Funding for this project was provided by a grant from the U.S. Department of Energy. J.B.J. was partially supported by a National Research Foundation of Korea Grant (NRF-2009-352-D00056). We also thank the groups of Prof. Pinyung Feng (University of California, Riverside) and Prof. Jongheop Yi (Seoul National University) for their help with the Brunauer–Emmett–Teller and thermal gravimetric analysis experiments.

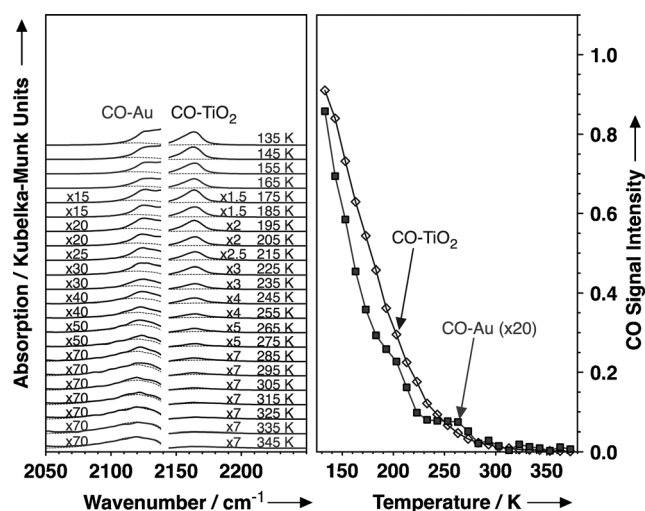


Figure 2. Left: In situ DRIFT spectra as a function of temperature for carbon monoxide adsorption on our Au@TiO₂ catalyst in the presence of gas-phase CO at 200 Torr. The contributions from gas-phase CO, determined by separate blank experiments, are shown by dotted lines. Right: Summary of the CO peak intensities versus temperature extracted from the data of the DRIFT spectra (left-hand panel). The extent of the CO adsorption on gold (CO–Au) and titania (CO–TiO₂) were estimated from the areas of the peaks in the 2090–2145 and 2145–2190 cm^{−1} regions, respectively.

can be identified in Figure 2, at 2090–2145 cm^{−1} and at 2145–2190 cm^{−1}, which we assign to CO adsorption on gold and on titania, respectively, based on data from blank experiments with pure titania and a 1 wt % Au/TiO₂-P25 catalyst (made out of ca. 10 nm gold nanoparticles dispersed on a Degussa titania P-25 powder; the TEM picture is provided in Figure 1e) as reference.^[14,15] The information on the evolution of the coverages of the two types of CO as a function of temperature extracted from these data is shown in the right-hand panel of Figure 2.

It is clear that, although most of the adsorption of CO takes place on the titania surface, some adsorption also occurs on the gold nanoparticles inside the shells. This adsorption is weak, hence the small blue-shift seen in the C–O bond-stretching frequency compared to that in gas-phase CO, but slightly stronger than on titania: a detectable peak for CO on gold is seen for temperatures up to approximately 270 K. The adsorption is also reversible: all IR signals for CO (including those for the CO on titania) go away upon pumping, and no adsorbed CO could be detected under vacuum following exposures to gas-phase CO at any temperature, down to 150 K (data not shown). It should also be noted that the low intensity of the IR signal for CO on gold relative to that on titania is to be expected given the low metal loading in these yolk@shell catalysts. Based on geometrical considerations, the total amount of gold in our catalyst is estimated to be about 0.2 wt %, and the Au-to-TiO₂ ratio of surface areas (not considering the porosity of the titania) approximately 0.1 %.

The performance of the Au@TiO₂ catalyst was also tested for the promotion of the oxidation of CO with O₂ at room temperature. The relevant data are reported in Figure 3. Both the CO coverages on the gold surface and the yields of the

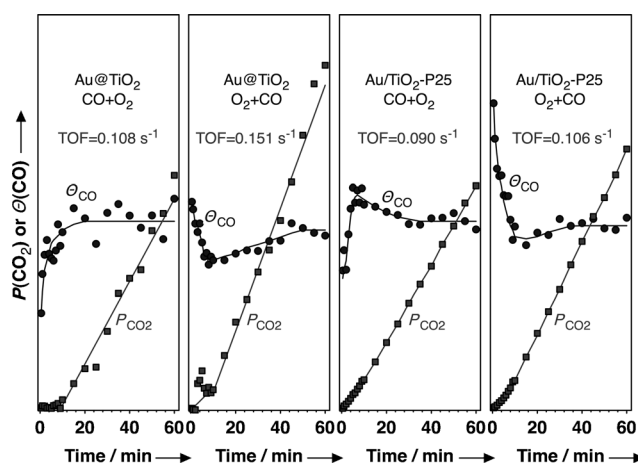


Figure 3. Time dependence of the carbon monoxide coverage on gold (θ_{CO} , circles) and the carbon dioxide partial pressure (P_{CO_2} , squares) during the room-temperature oxidation of CO with O₂ on gold/titania catalysts. The two left-hand panels correspond to our Au@TiO₂ yolk@shell catalyst, the two right-hand panels to a reference Au/TiO₂-P25 sample. The first and third panels were obtained by first introducing 200 Torr of CO into the cell and then adding 200 Torr of O₂; in the second and fourth panels the sequence was reversed. The coverage of CO on Au and the gas-phase CO₂ pressure were estimated from the integrated intensities of the DRIFT signals in the 2090–2145 and 2300–2400 cm^{−1} regions, respectively. Turnover frequencies (TOF), in units of molecules of CO₂ produced per surface Au atom per second, are also reported.

gas-phase CO₂ produced were followed as a function of reaction time in two sets of experiments in which CO and O₂ were added to the reaction vessel sequentially either in that order or in the reverse O₂ + CO sequence. Data are also reported from experiments with our reference Au/TiO₂-P25 catalyst for comparison. The integrated DRIFT intensities are reported in arbitrary units, but were normalized to the value for the steady-state coverage of CO on the gold surface.

The main observation from these data is that our Au@TiO₂ catalyst is indeed quite active in promoting the oxidation of carbon monoxide, displaying comparable reaction rates, relative to the exposed surface of the gold nanoparticles, to those obtained with the traditional Au/TiO₂-P25 catalyst. Turnover frequencies (TOF) of about 0.1 and 0.3 s^{−1} were measured at 300 and 325 K, respectively, from which an apparent activation energy of approximately 34 kJ mol^{−1} can be estimated. Our TOF values are larger than most of those reported with conventional supported catalysts,^[15,16] but slightly lower than those reported on model systems.^[8,17] The latter observation can be accounted for by the relatively large size of our gold nanoparticles, which have diameters outside the optimum range reported for these applications, and which, consequently, have a lower fraction of their Au atoms directly interacting with the titania surface.^[8] In any case, it can be safely said that our new yolk@shell nanoarchitecture does not hinder reactivity, since the TOFs measured with the Au@TiO₂ catalyst are, if anything, larger than those with our catalyst consisting of the same gold nanoparticles ($d = 10$ nm) dispersed on a regular P25 titania support; a direct comparison between

these two samples removes any effects caused by the Au–TiO₂ interface from the discussion. The surface areas of the titania support of both our samples, as determined by Brunauer–Emmett–Teller measurements using N₂, are also comparable, 57 and 59 m² g^{−1} for the nanoshells and the P25, respectively, a fact that eliminates the need to consider any effects caused by variations in porosity.

One interesting observation here is that, with the Au@TiO₂, an induction period of approximately 10 minutes is seen before CO conversion commences. This suggests that the reaction may be initially limited by diffusion of the reactants to the void volume inside the titania shells (although the time appears quite long for that). A transient is also observed in the CO coverage on gold, but that occurs in a shorter time frame and is also seen with the conventional Au/TiO₂-P25 catalyst, where no induction time for reaction is observed. The fact that the induction period is more noticeable in the experiment where oxygen is added last to the gas mixture suggests that oxygen diffusion through the titania shell may be slower than CO diffusion. It is also worth mentioning that high activity is seen with the Au@TiO₂ catalyst even at room temperature. This is in contrast with what has been reported for the performance of a Au@ZrO₂ catalyst, with which the onset for CO oxidation occurs around 450 K.^[18] This difference highlights the unique synergy of gold with titania.

Finally, the stability of the Au@TiO₂ catalyst was tested. No changes in weight were observed in the 300–1000 K temperature range in TGA experiments for either of our two catalysts, the Au@TiO₂ nanostructure or the reference Au/TiO₂-P25, other than those explained by the loss of adsorbed water. Moreover, based on TEM data, it was determined that the Au@TiO₂ catalyst remains virtually unchanged upon calcination at temperatures up to 775 K, both in terms of the size and shape of the gold nanoparticles and of the integrity of the titania shells (Figure 1 b,d). On the other hand, exposure of the reference Au/TiO₂-P25 catalyst to similar treatments results in significant sintering and in the formation of gold particles with diameters of up to approximately 50 nm (Figure 1 f). Calcination of the yolk@shell structures to higher temperatures does lead to a change in the texture of the shell material and to the shattering of a fraction of those structures, but even then only a small fraction (ca. 10 %) is affected (data not shown). We believe that this may be due to the formation of a sodium titanate phase during the etching step, and are working to minimize the problem.

In summary, a new Au@TiO₂ yolk@shell-nanostructured catalyst was prepared and characterized. This catalyst proved capable of adsorbing small gas molecules on the metal surface, and of promoting the oxidation of carbon monoxide at rates comparable to those seen with more conventional titania-supported gold catalysts. It was also shown that the new nanoarchitecture prevents the gold nanoparticles from sintering, making the new catalyst more stable. The use of titania as the shell material proved critical to achieve high reactivity at low temperatures, much higher than that reactivity seen with catalysts based on other oxides. Further studies are still needed to test the long-term stability of the Au@TiO₂ catalyst under reaction conditions.

Experimental Section

Au nanoparticle synthesis: An aqueous solution of HAuCl₄·3H₂O (2.54 M, 18 µL) was added to deionized water (30 mL) and heated to boiling point. A sodium citrate solution (3 wt %, 1 mL) was then added, and the resulting mixture was kept for 30 minutes under stirring. Upon cooling down to room temperature, the solution was mixed with an aqueous solution of polyvinylpyrrolidone (PVP, 12.8 mg mL^{−1}, 0.235 mL), and kept overnight to allow for the adsorption of PVP on the Au surface. The Au nanoparticles were separated from the solution by centrifugation, and redispersed in water (4 mL).

SiO₂ coating: The above-mentioned colloidal Au solution (1 mL) was sequentially mixed with water (3.3 mL), ethanol (23 mL), tetraethyl orthosilicate (TEOS, 0.86 mL), and an aqueous solution of ammonia (28 %, 0.62 mL). The reaction mixture was stirred for 4 h at room temperature, then the resulting Au@SiO₂ particles were centrifuged and washed three times with ethanol, and redispersed in ethanol (5 mL) under ultrasonication.

TiO₂ coating: The above-mentioned Au@SiO₂ particles were dispersed in a mixture containing hydroxypropyl cellulose (HPC, 100 mg), ethanol (20 mL), and water (0.1 mL). After the reaction mixture had been stirred for 30 minutes a solution of tetrabutyl titanate (TBOT, 1 mL) dissolved in ethanol (5 mL) was slowly added to the mixture using a syringe pump (0.5 mL min^{−1}). After injection, the temperature was increased to 358 K while the reaction mixture was stirred for 90 minutes under reflux conditions. The precipitate, which contained Au@SiO₂@TiO₂ nanocomposites, was collected using centrifugation, washed with ethanol, and redispersed in deionized water (20 mL).

SiO₂ etching: A NaOH solution (2.5 M, 1 mL) was added to the above-mentioned Au@SiO₂@TiO₂ solution, and the mixture was stirred for 6 h to selectively remove the silica. The resulting Au@TiO₂ yolk@shell particles were finally isolated by centrifugation and washed five times with deionized water.

DRIFT and catalysis: The infrared absorption data were acquired using a Bruker Tensor 27 FTIR interferometer and a Harrick variable-temperature Praying Mantis DRIFT reaction chamber. The catalysts were sequentially pretreated ex situ in flowing H₂ (775 K, 6 h), O₂ (675 K, 6 h), and H₂ again (475 K, 6 h) prior to their use. XRD measurements after catalytic reaction indicated that the shells were composed mainly of amorphous titania but also contained small portions of Na_{0.23}TiO₂, NaTi₈O₁₃, and TiO₂ anatase phases.

Received: December 7, 2010

Revised: January 26, 2011

Published online: April 6, 2011

Keywords: gold · heterogeneous catalysis · IR spectroscopy · nanostructures · titania

- [1] G. C. Bond, P. A. Sermon, G. Webb, D. A. Buchanan, P. B. Wells, *J. Chem. Soc. Chem. Commun.* **1973**, 444.
- [2] M. Haruta, N. Yamada, T. Kobayashi, S. Iijima, *J. Catal.* **1989**, *115*, 301.
- [3] M. Haruta, *Catal. Today* **1997**, *36*, 153.
- [4] A. S. K. Hashmi, G. J. Hutchings, *Angew. Chem.* **2006**, *118*, 8064; *Angew. Chem. Int. Ed.* **2006**, *45*, 7896.
- [5] G. C. Bond, C. Louis, D. T. Thompson, *Catalysis by Gold*, Imperial College Press, London, **2007**.
- [6] A. Corma, H. Garcia, *Chem. Soc. Rev.* **2008**, *37*, 2096.
- [7] V. Schwartz, D. R. Mullins, W. Yan, B. Chen, S. Dai, S. H. Overbury, *J. Phys. Chem. B* **2004**, *108*, 15782.
- [8] M. Chen, D. W. Goodman, *Chem. Soc. Rev.* **2008**, *37*, 1860.
- [9] P. V. Kamat, *J. Phys. Chem. C* **2007**, *111*, 2834.
- [10] J. Lee, J. C. Park, H. Song, *Adv. Mater.* **2008**, *20*, 1523.

- [11] Q. Zhang, I. Lee, J. Ge, F. Zaera, Y. Yin, *Adv. Funct. Mater.* **2010**, 20, 2201.
 - [12] I. Lee, M. A. Albiter, Q. Zhang, J. Ge, Y. Yin, F. Zaera, *Phys. Chem. Chem. Phys.* **2010**, 13, 2449.
 - [13] M. Ye, Q. Zhang, Y. Hu, J. Ge, Z. Lu, L. He, Z. Chen, Y. Yin, *Chem. Eur. J.* **2010**, 16, 6243.
 - [14] J.-D. Grunwaldt, A. Baiker, *J. Phys. Chem. B* **1999**, 103, 1002.
 - [15] Y. Denkwitz, B. Schumacher, G. Kučerová, R. J. Behm, *J. Catal.* **2009**, 267, 78.
 - [16] G. R. Bamwenda, S. Tsubota, T. Nakamura, M. Haruta, *Catal. Lett.* **1997**, 44, 83.
 - [17] K. Christmann, S. Schwede, S. Schubert, W. Kudernatsch, *ChemPhysChem* **2010**, 11, 1344.
 - [18] P. M. Arnal, M. Comotti, F. Schüth, *Angew. Chem.* **2006**, 118, 8404; *Angew. Chem. Int. Ed.* **2006**, 45, 8224.
-